Journal of Thermal Analysis, Vol. 33 (1988) 633–642

TEMPERATURE-DEPENDENCE OF INTERFACIAL ENERGIES BETWEEN SOLID OXIDE CERAMICS AND LIQUID METALS

P. Nikolopoulos, D. Sotiropoulou and *G. Ondracek**

INSTITUTE OF PHYSICAL METALLURGY, DEPT. OF CHEMICAL ENGINEERING, UNIVERSITY OF PATRAS, GR-26110 PATRAS, GREECE
* UNIVERSITÄT AND KERNFORSCHUNGSZENTRUM KARLSRUHE, D–7500 KARLSRUHE, G.F.R.

The interfacial energies between solid oxide ceramic and liquid metals have been investigated for a number of systems. At the metal melting point: (1) the interfacial energies between a given oxide ceramic and various metals vary by less than 10%:

$\gamma_{SL} = 2.538 \pm 0.139$ J/m^2 for Al_2O_3-liquid metals;
$\gamma_{SL} = 1.599 + 0.064$ J/m^2 for ZrO_2-liquid metals;
$\gamma_{SL} = 1.676 \pm 0.142$ J/m^2 for UO_2-liquid metals;

(2) the respective contact angles ($\Phi > 90°$) idicate no wettability. Linear temperature functions of the interfacial energies in oxide ceramic-liquid metal systems have been derived. By extrapolation, temperature coefficients of interfacial energies can be estimated for oxide ceramic-liquid metal systems that have not yet been measured. The interfacial energies, together with the surface energies of the materials concerned, also provide the work of adhesion for all Al_2O_3- and ZrO_2-liquid metal combinations considered.

As demonstrated in Fig. 1, composites and also composed materials result from combinations of phases taken from different main classes of materials, such as ceramics and metals (cerments), metals and polymers, polymers and ceramics, or even metals, ceramics and polymers. Composites in this context are understood to be multiphased (heterogeneous), or at least two-phased and macroscopically homogeneous. Macroscopically inhomogeneous combinations of phases (or constituents in the case of non-equilibrium), however, are defined as composed materials, referring, for example, to sandwich structures [12]. Composites (as well as composed materials) offer the possibility to construct tailor-made engineering materials with effective properties, which reflect the properties of their phases and the influence of the microstructure on the properties of the multphase materials [13]. As always in science and technology, however, this hold only for the if-then

John Wiley & Sons, Limited, Chichester
Akadémiai Kiadó, Budapest

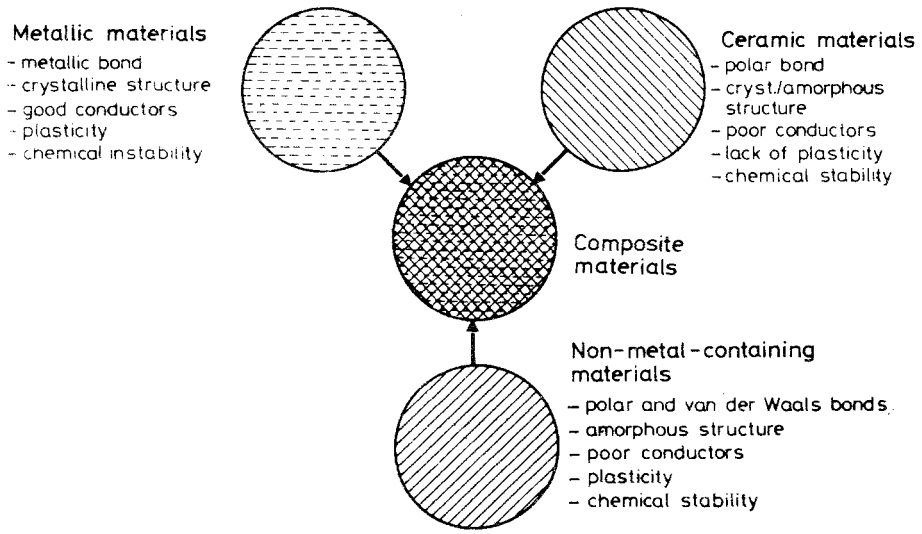

Fig. 1.

principle: *if bonding exists between the phases, then* (and only then) the realization of effective properties comes true!

The bonding problem is generally related to the interfacial energies, but is not restricted only to the solid state. Especially in the case of liquid-phase sintering (or "solid-phase melting"), wettability plays the key role in the obtaining of dense materials with desired microstructures, as in the case of hard metals, for example.

This is why the determination of interfacial energies between ceramics and liquid metal phases is of importance in the technology of cermets. Wetting in a solid-liquid-vapour system in thermodynamic equilibrium is characterized by the wetting angle. Its magnitude depends on the temperature and the surface, as well as on the interfacial energies of the phases in contact.

An established method for studying the interfacial phenomena involves a sessile drop of liquid metal lying on a substrate of the relevant metal oxide (Fig. 1). In this the following equation hold:

$$\gamma_{SV} = \gamma_{SL} + \gamma_{LV} \cos \Theta \tag{1}$$

where γ_{SV} and γ_{LV} are the surface energies of the solid and liquid phases, respectively, γ_{SL} is the solid-kiquid interfacial energy, and Θ is the wetting. The work of adhesion (W_a) is given by

$$W_a = \gamma_{LV}(1 + \cos \Theta) \tag{2}$$

In the present work, experiments are described which were carried out in order to determine the temperature functions of the interfacial energies in the Al_2O_3–Bi, –Pb, –Cu and –Ni and the ZrO_2–Cu, –Co and –Ni systems. Additional literature data on wetting angles in the systems Al_2O_3–Sn and Al_2I_3–Co [8] supplement the experimentally determined quantities.

Experimental procedure

Polycrystalline alumina AL23 (tradename of Friedrichsfels Co., FRG) with a purity of 99.7% and polycrystalline zirconia ZR23 (stabilized with 5 wt.% CaO) with a purity of 99%, were used in wetting experiments. The as-received Al_2O_3 had a density of 3.7 to 3.95 g cm^{-3}, whilst the ZrO_2 density was between 5.0 and 5.4 g cm^{-3}. In Al_2O_3 the grain sizes varied between 10 and 20 μm, and in ZrO_2 between 30 and 50 μm. Discs 20 mm in diameter and 3 mm in thickness were used in the experiments. The purity of the metals (Fa. Ventron GmbH, FRG) was 99.9985 wt.% for Sn, 99.99995 wt.% for Bi, 99.9985 wt.% for Pb, 99.999 wt.% for Cu, 99.99 wt.% for Ni and 99.998 wt.% for Co.

Purified argon was used as experimental atmosphere. The samples were heated with an induction coil and the wetting angles were measured from photographic projections of the sessile drops.

Experimental results

Wetting angles

Since the wetting angle (θ) in all the systems examined was greater than 90°, the sessile drop has a spheroidal form. From the values of X_{90}, Z_{90}, X_0 and Z_0 (Fig. 2) and by using the tables of Bashfort and Adams, the wetting angle can be determined [2, 9].

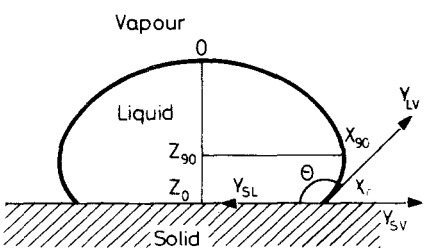

Fig. 2.

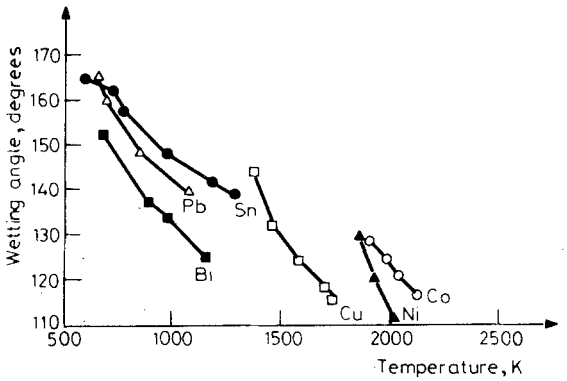

Fig. 3.

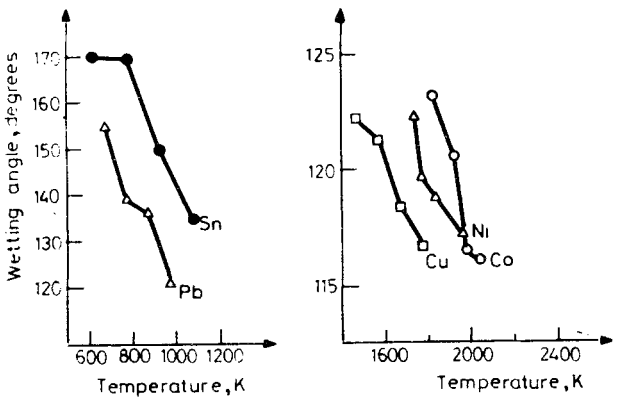

Fig. 4.

For each system and each temperature, two to four experiments were carried out, each lasting about 20–30 min. Photographs of the sessile drops were obtained at 5-min intervals, resulting in wetting angles finally being time-independent in all systems examined.

Figures 3 and 4 show the temperature-dependences of the wetting angles in the systems Al_2O_3–Sn, –Bi, –Pb, –Cu, –Ni and –Co and ZrO_2–Sn, –Pb, –Cu, –Ni and –Co, rspectively. The values of the measured wetting angles agree reasonably well with most of the literature data obtained for the systems under inert gas conditions. The results indicate that the liquid metals do not wet the ceramic oxides in the investigated temperature range. This is frequently attributed to the domination of the ceramic surface by oxygen anions. The wetting angle decreases with increasing temperature and melting point of the metal.

Moreover, the angles (θ) indicate that the wettability is not sufficient for the high densification of composites during liquid-phase sintering.

Interfacial energy and work of adhesion

The measured wetting angles in the Al_2O_3- and ZrO_2-liquid metal systems, together with literature data on the surface energies of solid ceramics (Al_2O_3 [8] and ZrO_2 [4]) and on the surface energies of liquid metals in an inert gas atmosphere or vacuum [1, 5–8], were used for calculation of the interfacial energies (Eq. (1)) and the work of adhesion (Eq. (2)).

In this context, the temperature coefficient of the energy of ZrO_2 was estimated as $d\gamma_{SV}/dT = -0.3 \cdot 10^{-3}$ J m^{-2} deg^{-1}, a value which compares well with the corresponding temperature coefficients of the oxides ThO_2 ($-0.24 \cdot 10^{-3}$ J m^{-2} deg^{-1}) and UO_2 ($-0.35 \cdot 10^{3}$ J m^{-2} deg^{-1}), which have similar crystal structures.

Table 1 lists the temperature functions of surface energies for all components. Since the metal vapour existing in the furnace atmosphere did not affect the surface energies or the values of the wetting angles appreciably, was decided to neglect this [3, 10].

Table 1 Linear temperature functions of surface energies for solid ceramics and liquid metals

Material	Surface energy (J·m^{-2})	
Al_2O_3	$2.559 - 0.784 \cdot 10^{-3}\ T$	$0 \leqslant T < 2323$ K
ZrO_2	$1.227 - 0.3 \cdot 10^{-3}\ T$	$0 \leqslant T < 2893$ K
Sn	$0.544 - 0.07 \cdot 10^{-3}\ (T - Tm)$	$T \geqslant T_m =$ 505 K
Bi	$0.372 - 0.09 \cdot 10^{-3}\ (T - Tm)$	$T \geqslant T_m =$ 544 K
Pb	$0.468 - 0.13 \cdot 10^{-3}\ (T - T_m)$	$T \geqslant T_m =$ 600 K
Cu	$1.311 - 0.20 \cdot 10^{-3}\ (T - T_m)$	$T \geqslant T_m =$ 1356 K
Ni	$1.754 - 0.28 \cdot 10^{-3}\ (T - T_m)$	$T \geqslant T_m =$ 1726 K
Co	$1.610 - 0.29 \cdot 10^{-3}\ (T - T_m)$	$T \geqslant T_m =$ 1768 K

The results of the measurements of the wetting angles, as well as the calculated values of the work of adhesion and the interfacial energies in the investigated systems, are in Tables 2 and 3. Table 4 shows the linear temperature functions of the interfacial energies and the coefficients of correlation. In Figs 5 and 6 the data on the interfacial energies of Al_2O_3-liquid metals and ZrO_2-liquid metals, respectively, are plotted *vs.* the homologous temperature (T/T_m). These Figures, together with Table 4, clearly indicate what was expected from earlier experiments on the of interfacial energies of UO_2-liquid metals (compare Fig. 7 [11]): at the melting points of the metals, the

Table 2 Wetting angles (Θ), work of adhesion (W_a), interfacial energies (γ_{sL}) in the Al_2O_3-liquid metal systems

System	T, K	Θ, deg	Standard deviation	W_a, $J \cdot m^{-2}$	γ_{SL}, $J \cdot m^{-2}$
Al_2O_3–Sn	611	165.24	±4.06	0.018	2.599
	726	161.74	±2.68	0.027	2.492
	772	157.74	±7.86	0.039	2.440
	975	148.26	±4.37	0.076	2.230
	1183	141.96	±1.71	0.106	2.023
	1280	138.95	±2.67	0.120	1.925
Al_2O_3–Bi	689	152.73	±4.95	0.040	2.338
	890	137.38	±2.99	0.090	2.112
	965	134.33	±1.90	0.101	2.035
	1144	125.24	±1.86	0.135	1.845
Al_2O_3–Pb	667	165.30	±3.05	0.015	2.480
	711	160.48	±7.15	0.026	2.430
	860	149.00	±5.18	0.062	2.257
	1073	139.82	±10.05	0.096	2.029
Al_2O_3–Cu	1370	143.87	±2.82	0.252	2.541
	1450	131.86	±2.66	0.430	2.284
	1575	123.97	±2.30	0.559	2.032
	1695	118.42	±1.42	0.651	1.822
	1720	116.10	±1.19	0.693	1.756
Al_2O_3–Ni	1843	129.28	±2.98	0.631	2.204
	1908	121.20	±1.34	0.821	1.945
	2003	111.30	±0.66	1.067	1.598
Al_2O_3–Co	1888	128.20	±2.81	0.601	2.053
	1973	123.91	±2.12	0.686	1.877
	2023	120.10	±1.53	0.766	1.743
	2113	116.68	±0.88	0.832	1.580

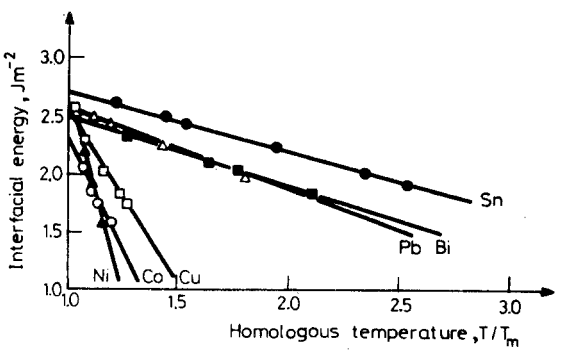

Fig. 5.

Table 3 Wetting angles (Θ), work of adhesion (W_a). interfacial energies (γ_{SL}) in the ZrO_2-liquid metal systems

System	T, K	Θ, deg	Standard deviation	W_a, $J \cdot m^{-2}$	γ_{SL},
ZrO_2–Sn	623	170.04	±0.63	0.008	1.568
	773	169.40	±0.88	0.009	1.511
	923	149.73	±5.93	0.070	1.395
	1073	134.92	±2.87	0.148	1.261
ZrO_2–Pb	673	154.88	±2.73	0.043	1.441
	773	139.73	±0.87	0.106	1.335
	873	136.36	±0.53	0.120	1.278
	973	121.55	±3.81	0.200	1.155
ZrO_2–Cu	1473	122.18	±1.28	0.602	1.471
	1573	121.31	±2.43	0.609	1.414
	1673	118.38	±1.09	0.655	1.318
	1773	116.73	±2.07	0.676	1.247
ZrO_2–Ni	1740	122.33	±0.81	0.814	1.641
	1773	119.71	±1.85	0.878	1.558
	1833	118.82	±1.65	0.893	1.508
	1953	117.15	±1.69	0.919	1.412
ZrO_2–Co	1823	123.21	±1.78	0.721	1.553
	1923	120.38	±0.57	0.774	1.441
	1973	116.53	±0.69	0.858	1.328
		116.06	±0.52	0.858	1.226

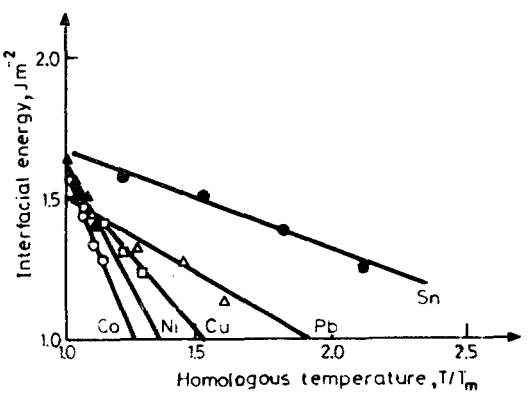

Fig. 6.

Table 4 Linear temperature functions of the interfacial energy $|\gamma_{SL}(T) = \gamma_{SL}(T_m) - d\gamma_{SL}/dT(T-T_m)|$ in the Al_2O_3- and ZrO_2-liquid metal systems (R = correlation coefficient)

System		Interfacial energies, $J \cdot m^{-2}$	R
Al_2O_3	–Sn	$2.710 - 1.014 \cdot 10^{-3}$ (T–505)	0.9999
	–Bi	$2.492 - 1.083 \cdot 10^{-3}$ (T–544)	0.9998
	–Pb	$2.552 - 1.112 \cdot 10^{-3}$ (T–600)	0.9998
	–Cu	$2.528 - 2.141 \cdot 10^{-3}$ (T–1356)	0.9943
	–Ni	$2.641 - 3.778 \cdot 10^{-3}$ (T–1726)	0.9997
	–Co	$2.305 - 2.126 \cdot 10^{-3}$ (T–1768)	0.9978
ZrO_2	–Sn	$1.671 - 0.691 \cdot 10^{-3}$ (T–505)	0.9857
	–Pb	$1.506 - 0.915 \cdot 10^{-3}$ (T–600)	0.9914
	–Cu	$1.568 - 0.768 \cdot 10^{-3}$ (T–1356)	0.9957
	–Ni	$1.628 - 0.992 \cdot 10^{-3}$ (T–1726)	0.9715
	–Co	$1.622 - 1.274 \cdot 10^{-3}$ (T–1768)	0.9818

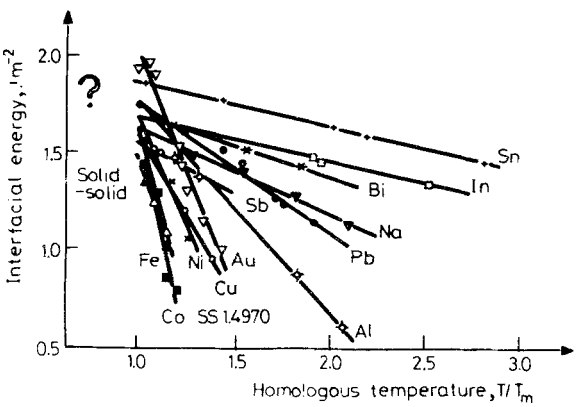

Fig. 7.

interfacial energies with a given ceramic substrate vary in a restricted region, no matter what type of metal is concerned. The mean values and the standard deviations of these interfacial energies are $\gamma_{SL} = 2.538 \pm 0.139$ J·m^{-2} for Al_2O_3-liquid metals systems, and $\gamma_{SL} = 1.599 \pm 0.064$ J·m^{-2} for ZrO_2-liquid metal systems, which compares reasonably well with the literature data for the UO_2-liquid metal systems [11] (compare Fig. 7): $\gamma_{SL} = 1.676 \pm 0.142$ J·m^{-2}.

This justifies the conclusion that the use of an average value for the interfacial energy between one ceramic material and various liquid metals at the melting point of the metal allows a reasonable approach to the wettability in these systems, independently of the type of the metal it applies in particular, for those metals with high melting points and high surface energies.

* * *

The present work was performed in the frame of bilateral German–Greek cooperation in science and technology. It was sponsored financially by the Deutsche Forschungsgemeinschaft Bonn and supported by the Internationales Büro, Kernforschungsanlage Jülich. The authors gratefully acknowledge this assistance.

References

1 B. C. Allen, "Liquid Metals" ed. by S. Z. Beer (Dekker, New York, 1972) p. 161.
2 F. Bashfort, S. C. Adams, "An attempt to test the theories of capillary actions" (University Press, Cambridge, 1883) p. 63.
3 T. Inoue, H. Matzke, J. Amer. Ceram: Soc. 64 (1981) 355.
4 W. D. Kingery, J. Amer. Ceram. Soc. 37 (1954) 42.
5 G. Lang, P. Laty, J. Ch., Joud, P. Desré, Z. Metallkunde 68 (1977) 113.
6 G. Lang, Z. Metallkunde 67 (1976) 549.
7 A. R. Miedema, R. Boom, Z. Metallkunde 69 (1978) 123.
8 P. Nikolopoulos, J. Mater. Sci. 230 (1985) 3993.
9 P. Nikolopoulos, G. Ondracek, Z. Werkstofftechnik 13 (1982) 60.
10 P. Nikolopoulos, S. Nazaré, F. Thümmler, J. Nucl. Mater., 71 (1977) 89.
11 P. Nikolopoulos, G. Ondracek, J. Nucl. Mater., 98 (1981) 306.
12 G. Ondracek, Umschau 85–7 (1985) 400.
13 G. Ondracek, Mat. Chemistry and Physics 15 (1986) 281.

Zusammenfassung — Grenzflächenenergien zwischen festen Oxidkeramiken und flüssigen Metallen wurden für eine Reihe von Systemen untersucht. Beim Schmelzpunkt des Metalls: (1) variieren die Grenzflächenenergien γ_{SL} zwischen einer Keramik und verschiedenen Metallen um weniger als 10%: für

Al_2O_3 – Metall $\gamma_{SL} = (2.538 \pm 0.139)\ J \cdot m^{-1}$
ZrO_2 – Metall $\gamma_{SL} = (1{,}599 \pm 0{,}064)\ J\ m^{-2}$
UO_2 – Metall $\gamma_{SL} = (1{,}676 \pm 0{,}142)\ J\ m^{-2}$

(2) zeigen die Kontaktwinkel ($> 90°$) keine Benetzung.
Die Grenzflächenenergien in Oxidkeramik-Metallschmelze-Systemen hängen linear von der Temperatur ab. Temperaturkoeffizienten der Grenzflächenenergien nicht untersuchter Keramik-Metallschmelze-Systeme lassen sich durch Extrapolation ermitteln. Aus den Grenzflächenenergien und den Oberflächenenergien der beteiligten Materialen wird die Adhäsionsarbeit für die untersuchten Al_2O_3- bzw. ZrO_2-Metallschmelze-Systeme erhalten.

Резюме — Для ряда систем были исследованы энергии поверхности раздела между твердотельной оксидной керамикой и жидкими металлами. Установлено, что в точке плавления металла энергии поверхности раздела оксидной керамики и различных металлов изменяются менее, чем на 10%:

$\gamma_{SL} = 2{,}538 \pm 0{,}139$ дж · м$^{-2}$ для системы Al_2O_3 — жидкие металлы
$\gamma_{SL} = 1{,}599 \pm 0{,}064$ дж · м$^{-2}$ для системы ZrO_2 — жидкие металлы
$\gamma_{SL} = 1{,}676 \pm 0{,}142$ дж · м$^{-2}$ для системы UO_2 — жидкие металлы

Указаны соответствующие контактные углы ($\Phi > 90°$) несмачиваемости.
Установлены линейные температурные зависимости энергии поверхности раздела в системах оксидная керамика — жидкий металл. Методом экстраполяции быть установлены температурные коэффициенты энергий поверхности раздела для неизмеренных до настоящего времени систем оксидная керамика — жидкий металл. Значения энергии поверхности раздела вместе с поверхностной энергией этих материалов предоставляют данные по адгезии для всех комбинаций оксидная керамика — жидкий металл.